

# Some details on state space smoothing using the conditional particle filter<sup>★</sup>

Andreas Svensson<sup>\*</sup> Thomas B. Schön<sup>\*</sup> Manon Kok<sup>\*\*</sup>

<sup>\*</sup> Department of Information Technology, Uppsala University, Sweden  
(e-mail: {andreas.svensson, thomas.schon}@it.uu.se)

<sup>\*\*</sup> Division of Automatic Control, Linköping University, Sweden  
(e-mail: manon.kok@liu.se)

---

**Abstract:** This technical report gives some additional details on the numerical examples used in Svensson et al. (2015).

---

## 1. INTRODUCTION

This report contains some details on the examples presented by Svensson et al. (2015). The problem under consideration is that of state space smoothing using the conditional particle filter with ancestor sampling (CPF-AS). In this report, we will address additional details concerning

- i) the simulated nonlinear, multimodal example used in Section 4.2.
- ii) the indoor positioning application used in Section 5.

Matlab code for the simulated example can be found via the first author's homepage.

## 2. SIMULATED NONLINEAR, MULTIMODAL EXAMPLE

This section gives an extended introduction to the problem considered in Svensson et al. (2015, Section 4.2). The essential details are contained in the original article, but we will provide an alternative introduction. The state space model considered in the problem is

$$x_{t+1}|x_t \sim \mathcal{N}(x_t, 0.5), \quad (1a)$$

$$y_t|x_t \sim g(y_t|x_t), \quad (1b)$$

$$x_1 = 3. \quad (1c)$$

The problem concerns smoothing for a given output sequence  $y_{1:t}$ . Thus we write  $G(x_t) \triangleq g(y_t|x_t)$ , the likelihood of  $x_t$ , omitting the dependence on  $y_t$ .  $G(x_t)$  is defined by the surface of Figure 1, which is parametrized as a sum of six Gaussian-like functions. The specific parametrization is found in the provided source code.

The state space filtering/smoothing problem arising from this problem is solved using three approaches. For filtering, the particle filter in Svensson et al. (2015, Algorithm 1), with  $q_t = f$ , is used. For smoothing, the FFBSi with rejection sampling, as presented in Lindsten and Schön (2013, Algorithm 5), is used, together with the MCMC smoother in Svensson et al. (2015, Algorithm 3), and the results reported by Svensson et al. (2015) are obtained.

---

<sup>★</sup> This work was supported by the project *Probabilistic modelling of dynamical systems* (Contract number: 621-2013-5524) funded by the Swedish Research Council (VR) and CADICS, a Linnaeus Center, funded by the Swedish Research Council (VR).

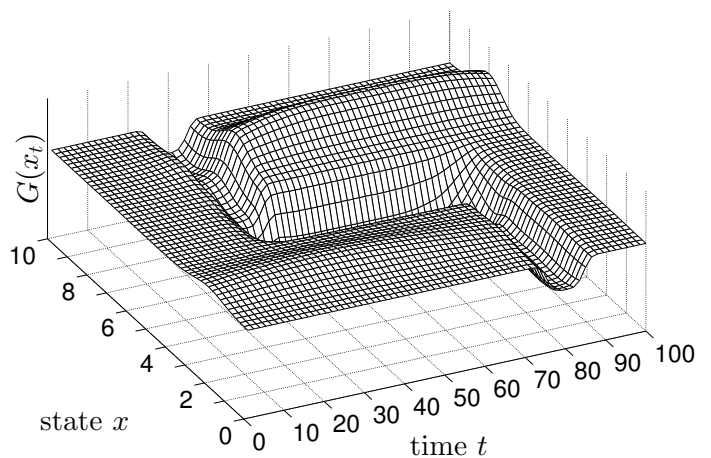


Fig. 1. Definition of  $G(x_t)$ .

## 3. INDOOR POSITIONING

This section focuses on the indoor positioning application in Svensson et al. (2015, Section 5). The problem is discussed in Kok et al. (2015), and concerns a sensor fusion problem involving accelerometer, gyroscope, and ultrawideband (UWB) measurements. There are several details on the problem not covered by Svensson et al. (2015); the non-uniform sampling intervals of the UWB measurements, the unknown transmission times, the sensor biases, some issues on the ancestor sampling, and the initialization of the first conditional trajectory.

We repeat the state space model here:

$$\left. \begin{aligned} p_{t+1}^n &= p_t^n + T_s v_t^n + \frac{T_s^2}{2} a_t^n, \\ v_{t+1}^n &= v_t^n + T_s a_t^n, \\ q_{t+1}^{nb} &= q_t^{nb} \odot \exp \frac{T_s}{2} \omega_t, \end{aligned} \right\} f(x_{t+1}|x_t, a_t^n, \omega_t) \quad (2a)$$

$$y_{m,t} = \tau_t + \|r_m^n - p_t^n\|_2 + e_{m,t} \quad \} g(y_t|x_t), \quad (2b)$$

with the same notation as Svensson et al. (2015). Most important,  $x_t^T = [(p_t^n)^T (v_t^n)^T (q_t^{nb})^T]$  forms the state vector, and  $a_t^n$  are the acceleration,  $\omega_t$  the angular velocity, and  $y_{m,t}$  are the UWB measurements (for receiver number  $m$ ). The sampling frequency for the accelerometers and the gyroscopes is 120 Hz.

The acceleration and angular velocity are modeled to be measured as

$$y_{a,t} = R_t^{bn}(a_t^n - g^n) + \delta_a + e_{a,t}, \quad (3)$$

$$y_{\omega,t} = \omega_t + \delta_\omega + e_{\omega,t}. \quad (4)$$

with notation as Svensson et al. (2015). Through the measurement noise in these models, stochastic noise enters the state space.

### 3.1 Non-uniform sampling interval

For every sampling step  $t$ , the accelerometer and gyroscope data  $y_{a,t}$  and  $y_{\omega,t}$  are available. However, the UWB measurements are recorded at a lower sampling rate, and are available only for approximately every tenth sample. A high level algorithm illustrating how this is handled is shown in Algorithm 1.

---

**Algorithm 1** Algorithmic strategy for the indoor positioning problem

---

```

1: for  $k = 1, \dots, K$  do
2:   Sample  $x_1^i$  from  $q_1(x_1)$ 
3:   Draw  $x_1^i \sim p(x_1^i), i \in [1, N - 1]$ .
4:   Set  $x_{1:T}^N = x_{1:T}^{[k]}$ .
5:   for  $t = 1, \dots, T - 1$  do
6:     if UWB measurement  $\{y_{m,t}\}_{m=1}^M$  available then
7:       Set  $w_t^i = g(y_t|x_t^i), i \in [1, N]$ .
8:       Draw  $b_t^i$  with  $\mathbb{P}(b_t^i = j) \propto w_{t-1}^j, i \in [1, N - 1]$ .
9:       Set  $x_{1:t}^i = \{x_{1:t-1}^i, x_t^i\}, i \in [1, N - 1]$ .
10:    end if
11:    Draw  $x_{t+1}^i$  from  $f(x_{t+1}^i|x_t^i, a_t, \omega_t), i \in [1, N - 1]$ .
12:    Draw  $b_{t+1}^i$  with  $\mathbb{P}(b_{t+1}^i = j) \propto f(x_{t+1}^i|x_t^i)$ .
13:    Set  $x_{1:t+1}^N = \{x_{1:t}^N, x_{t+1}^N\}$ .
14:  end for
15:  Draw  $J$  with  $\mathbb{P}(i = J) \propto \frac{1}{N}$  and set  $x_{1:T}^{[k+1]} = x_{1:T}^J$ .
16: end for

```

---

(Note that the notation for the ancestor sampling variable is  $b$ , instead of  $a$ , not to confuse it with the accelerometer data.)

### 3.2 Unknown transmission times

When evaluating (2b), the transmission time  $\tau_t$  is unknown. It is approximately handled by Monte Carlo integration:

$$g(y_t|x_t) = p_e(y_{m,t} - \tau_t - \|r_m^n - p_t^n\|_2 | \tau_t) \tilde{\omega} \sum_j p_e(y_{m,t} - \tau_t^j - \|r_m^n - p_t^n\|_2), \quad (5)$$

where  $p_e$  is the pdf defined by eq. (11) in Svensson et al. (2015), and  $\tau_t^j$  are samples with possible values of  $\tau$ . All particles (indexed with  $i$ ) are evaluated with the same set of samples  $\tau_t^j$ .

### 3.3 Sensor bias

The numerical values of the sensor biases  $\delta_a$  and  $\delta_\omega$  are small, compared to the noise levels. They were therefore approximated manually. However, a more thorough system identification approach can be applied within the CPF-AS framework, as proposed by Lindsten (2013).

### 3.4 Evaluation of $f(x_{t+1}|x_t, a_t^n, \omega_t)$

For the ancestor sampling in Step 1 in Algorithm 1,  $f(x_{t+1}|x_t, a_t^n, \omega_t)$  needs to be evaluated. This involves the quaternion product and vector exponential in (2a), which can be manipulated as follows:

$$q_{t+1}^{nb} = q_t^{nb} \odot \exp \frac{T_s}{2} (\omega_t + e_{\omega,t}) \Leftrightarrow e_{\omega,t} = \frac{2}{T_s} \log ((q_t^{nb})^{-1} \odot q_{t+1}^{nb}) - \omega_t \quad (6)$$

where  $\log$  denotes the logarithm for unit quaternions (Hol, 2011). An approximation of this expression was used in the computations.

### 3.5 Low chance of ‘new ancestor’

One challenge is the small uncertainty in the position (2a), because of the (physically reasonable) factor  $\frac{T_s^2}{2}$  ( $\approx 10^{-5}$ ) in front of the noise term. To handle this, the uncertainty was artificially increased in the ancestor sampling step. This causes a substantial increase in the mixing, but also a non-feasible ‘jump’ in the smoothing trajectories. These artificial ‘jumps’ appears, however, to be rare and can also be expected to ‘even out’ as  $K \rightarrow \infty$ , but might indeed cause an overestimate of the variance.

A more thorough treatment would be to apply the recent development by Lindsten et al. (2015).

### 3.6 Initialization

The model has a state space of 9 dimensions (parametrized using 10 variables). The structure of the model and the uncertainties cause, according to our experience, the particle filter to diverge quickly if  $N$  is not sufficiently large. To speed up the initialization phase, a more ‘loose’ model was used in the first run of the CPF-AS to find one reasonable trajectory. This non-diverging trajectory was then used as the conditional trajectory for the subsequent run with the correct model.

## REFERENCES

- Hol, J.D. (2011). *Sensor Fusion and Calibration of Inertial Sensors, Vision, Ultra-Wideband and GPS*. Ph.D. thesis, Linköping University, Sweden.
- Kok, M., Hol, J.D., and Schön, T.B. (2015). Indoor positioning using ultrawideband and inertial measurements. *IEEE Transactions on Vehicular Technology*, 64(4), 1293–1303.
- Lindsten, F. (2013). An efficient stochastic approximation EM algorithm using conditional particle filters. In *Proceedings of 38th IEEE International Conference Acoustics, Speech, and Signal Processing (ICASSP)*, 6274–6278. Vancouver, Canada.
- Lindsten, F., Bunch, P., Singh, S.S., and Schön, T.B. (2015). Particle ancestor sampling for near-degenerate or intractable state transition models. *arXiv preprint arXiv:1505.06356*.
- Lindsten, F. and Schön, T.B. (2013). Backward simulation methods for Monte Carlo statistical inference. *Foundations and Trends in Machine Learning*, 6(1), 1–143.
- Svensson, A., Schön, T.B., and Kok, M. (2015). Nonlinear state space smoothing using the conditional particle filter. In *Proceedings of the 17th IFAC Symposium on System Identification (SYSID)*. Beijing, China.